Hindawi
Shock and Vibration
Volume 2019, Article ID 6325472, 13 pages
https://doi.org/10.1155/2019/6325472

Research Article

Study on the Vibroimpact Response of the Particle Elastic Impact on the Metal Plate

Yang Yang and Lirong Wan

College of Mechanical and Electronic Engineerings, Shandong University of Science and Technology, Qingdao 266590, China

Correspondence should be addressed to Lirong Wan; lirong.wan@sdust.edu.cn

Received 14 June 2019; Revised 30 August 2019; Accepted 9 September 2019; Published 20 October 2019

Academic Editor: Andrea Spaggiari

In order to study the contact and vibration response in the reciprocating impact between coal gangue particles and metal plate, on the basis of the Hertz contact theory, L-N contact model, and the Lagrange equation, this paper established an impact-contact model when the particles free falling to vertically impacts on the metal plate. The variable damping simulation method is proposed, and the accuracy of the variable damping simulation in the medium reciprocating collision is verified by combining the constant damping simulation, the variable damping simulation, and the falling body impact-contact model. The functional relationship between the damping term and the initial impact velocity in Adams simulation is also obtained. Then, through the rigid-flexible coupling method which is combined by Adams and Hypermesh, the three types of variable damping simulations are conducted: the simulation that the free-falling rigid rock sphere impact on the rigid metal plate, the simulation that the elastic rock sphere impact on the rigid metal plate, and the simulation that the elastic rock sphere impact on the elastic metal plate, respectively. Furthermore, contact and vibrate responses of the rock sphere and the metal plate in the three types of the simulation are studied. The results show that the impact-contact response of the rock sphere obtained from the simulation that the elastic rock sphere impact on the elastic metal plate is more accurate. After the flexible treatment of the rock sphere and the metal plate, most of the system energy is consumed during the impact. The conclusions will provide a theoretical calculation method for the medium vertical reciprocating impact and a theoretical basis for the setting of the damping term in Adams simulation and support the research basis for the study of the impact behavior between coal gangue particles and the metal plate.

1. Introduction

Coal plays a leading role in China's energy resources among which the thick coal seam accounts for nearly half of coal reserves [1]. With technology of full-mechanized top-coal caving, a great majority of the thick coal seam are exploited. In the mining of top-coal caving, plenty of coal gangue particles slip from the top of the hydraulic powered support and then fell onto the scraper conveyor through the cover beam and the tail beam. In the process, single impact or multiple impacts between particles can be produced, as well as between particles and the metal plate of the hydraulic powered support. As the digital mine construction and the coal gangue interface identification technology based on the vibration signal of tail beam demands, the research on the vibration signal and impact response caused by mechanical behavior of impact-contact between coal gangue and the metal plate of the hydraulic powered support has become an important project, which is of great significance to the development of coal mining modernization.

For the collision behaviors between the coal gangue particles and the impact-contact problems between the coal gangue particles and the hydraulic support metal plate, through the theories, simulations and experiments [2–19], and other methods, many scholars have carried out similar studies on the contact behavior between particles [20] and the contact behavior between particles and plates [21–25] in the early stage, which provides the basis for the research of the collision behavior between coal gangue particles or between the coal gangue and the hydraulic support in the

top-coal caving. Jackson et al. [26] investigated the restitution coefficient of the impacting elastic-perfectly plastic spheres. Zhao et al. [27] studied the elastic-plastic contact behavior with the FE model in the contact process of the power-law hardening elastic-plastic sphere and a rigid flat. Thornton [28] provided the analytical solution of the restitution coefficient in the normal contact interaction of two elastic-perfectly plastic spheres. Jamari and Schipper [29] put forward to an elastic-plastic contact model of ellipsoid bodies and studied the relationship of the contact parameters. Du and Wang [30] established a piecewise mechanical model of elastoplastic impact between two particles and simulated its impact process by using the finite element method. Vu-Quoc et al. [31] presented the data obtained from numerical experiments and established the normal and tangential elastoplastic force-displacement (FD) models in the impact of spheres. Based on Hertz contact theory and elastoplastic strengthening theory, He et al. [32] built the elastoplastic impact model of particles under the quasi-static condition. In addition, Krijt et al. [33] conducted researches on energy dissipation in head-on impacts of spheres, they present a new impact model that treats adhesion and viscoelasticity self-consistently, while energy losses arising from plastic deformation are assumed to be additive. Kligerman et al. [34] studied the unloading process when the elastic-plastic loaded sphere contacts with the rigid flat. Ovcharenko et al. [35] experimentally investigated the contact area between the sphere and the flat during loading, unloading, and cyclic loading. Through the theoretical contact model and the finite element contact simulation when the rock impacts on the metal plate with the consideration of the material damage, Zeng et al. [36] investigated the contact response when coal gangue impact on the metal plate which is supported by the screws. Cermik et al. [37] has conducted the research on the oblique impact of an elastic sphere with a rigid flat and the normal contact force as a function of deflection has been studied for different cases. Yang et al. [38] conducted the coal gangue impacting the metal plate experiment and studied the coal gangue recognition based on the test signal and the machine learning algorithms. All of these studies above will be guidance or references for the research on the impact behavior between particles and the metal plate of the hydraulic powered support in the top-coal mining. But for now, they mainly focus on the single impact between particles and the plates as well as the vibroimpact response in the process of impact-contact, there are few researches on the global repeated impact collision between the falling body and the plate or the setting of the damping term in the contact simulation process. Kadin et al. [39, 40] studied the multiple repeated loading and unloading of an elastic-plastic sphere and a rigid flat and investigated the evolution of the load-approach curves for the elastic-plastic spherical contact during its cyclic loading-unloading. However, the cyclic loading-unloading process did not mean the reciprocation of shock and rebound between objects in the gravitational space. The change of the contact damping caused by the changes of the contact velocity has also not been further explored. In addition, though the microscopic parameters in the impact-contact process such as the contact stress and contact strain can be extracted in the previous study through the finite element method, the research on the properties of macrokinetics is still weak.

On account of the results and deficiencies of above researches and on the basis of Hertz contact model and L-N contact model, the falling body impact-contact dynamics model when the particles repeated impact the metal plates, in combination with the Lagrange equation, is established in this paper. Through the comparative analysis between the results of Adams' rigid simulation and theory model, the functional relationship between the damping term and the initial impact velocity in Adams simulation can be obtained. Based on this, the dynamics simulation software Adams is combined with the finite element software Hypermesh to perform three types of variable damping simulations, which is rigid simulation that free-falling rigid rock sphere impacts the rigid metal plate (Type 1 simulation), the simulation that the elastic rock sphere impacts the rigid metal plate (Type 2 simulation), and the simulation that the elastic rock sphere impacts elastic metal plate (Type 3 simulation), respectively. Finally, the vibroimpact response and energy conversion of rock spheres and the vibroimpact response of the metal plate are studied.

The remainder of the paper is organized as follows: Section 2 establishes the falling body impact-contact dynamics model when the particles repeatedly impact the metal plate. Section 3 performs the Adams simulation when the metal plate is rigidly impacted by the rock sphere and determines the functional relationship between damping term and the initial impact velocity. Section 4 carries out three types of variable damping simulation when the free-falling rock sphere impacts the metal plate. Then, Section 5 analyzes the vibroimpact response and energy conversion of the rock sphere and vibration response of the metal plates in three types of simulation. Lastly, Section 6 shows some related work and conclusions.

2. Falling Body Impact-Contact Dynamics Model

2.1. Contact Force Model. According to Hertz contact law [41], the relationship between contact force P and the deformation of the sphere δ in the process of elastic sphere impacting the rigid flat surface may be written in the following form:

$$P = K \cdot \delta^n, \tag{1}$$

$$\delta = \left(\frac{5mv^2}{4K}\right)^{2/5}, \tag{2}$$

$$K = \frac{4\sqrt{3}}{3} \cdot E, \tag{3}$$

$$E = \frac{1-\mu_1^2}{E_1} + \frac{1-\mu_2^2}{E_2}, \tag{4}$$

where K is the contact stiffness of the system; E is the equivalent elastic modulus of the system; E_1, μ_1, E_2, and μ_2 are the elastic modulus and Poisson's ratio of elastic sphere and rigid flat surface; m is the mass of elastic sphere; n is the nonlinearity coefficient; and it is 3/2 for the vertical impact-contact of elastic sphere and rigid flat horizontal surface.

Based on Hertz contact law, the L-N model [42, 43] was proposed by Lankarani and Nikravesh. As a nonlinear viscoelastic model, the L-N model is one of the most popular and straightforward contact force model, which is in well conformity to experimental results and is valid for the cases in which the dissipated energy during the contact process is relatively small in comparison to the maximum absorbed elastic energy. So, the L-N contact model is selected in this paper. The model can be expressed as follows:

$$P = K \cdot \delta^n + D \cdot \dot{\delta}, \tag{5}$$

where D is the damping coefficient, $D = ((3K \cdot (1 - e_h^2))/4\dot{\delta}_0) \cdot \delta^n$, $\dot{\delta}_0$ is the initial velocity of elastic sphere, $\dot{\delta}$ is the velocity of sphere, and e_h is the restitution coefficient.

2.2. Analysis of the Falling Body Movement Processes. As shown in Figure 1, the coal-rock sphere falls freely from the height of h with the acceleration of g. It recovers and separates from the metal plate under the contact force after its impact and compression to the lowest point. In addition, it fails to take the friction between the rock sphere and the metal plate into consideration; therefore, the rock sphere will move up and slow down vertically with the acceleration of $-g$ at one separation speed. When it reaches the second highest point of h_1, the rock ball repeats the alternate movement in three stages of the free-falling body, impact-contact, and upward movement with a slower speed. After i time of impacts, the rock sphere, which is rebounded to the high point, shows that the height of the center of the sphere is h_i. And due to the effect of the system damping, $h_i < h_{i-1}$ ($i \geq 2$) during the whole movement. In the process of free-falling body and upward deceleration, the system is only influenced by gravity, and the interaction force between the rock sphere and the metal plate shows zero. In the process of impact-contact, the rock sphere is simultaneously influenced by gravity and contact force. And at this time, the contact force is calculated by the L-N model selected in this paper.

2.3. Falling Body Impact-Contact Model. As shown in Figure 2, the acceleration of g (gravity) is 9.8 m/s^2 when the downward movement is considered as the positive direction. It is assumed that the initial distance between the center of the sphere and the upper surface of the metal plate is h, the coordinate of the spherical motion is e, the radius of the rock sphere is R, and the compression of the rock sphere is δ; then, we obtain that

$$\begin{cases} \delta = h - R - e, & e > h - R, \\ \delta = 0, & e < h - R. \end{cases} \tag{6}$$

From equation (5), the contact force between the rock sphere and the metal plate is

$$F_n = \begin{cases} -\left[K \cdot \delta^n + K \cdot \delta^n \cdot \dfrac{3(1 - e_h^2)}{4\delta_{i0}'} \cdot e' \right], & \delta \neq 0, \\ 0, & \delta = 0. \end{cases} \tag{7}$$

The initial position of the center of the sphere is considered as the 0 potential energy point, and there is

$$\begin{cases} T = \dfrac{1}{2} m_1 v^2 = \dfrac{1}{2} m_1 (e')^2, \\ U = -m_1 g e - m_2 g h, \end{cases} \tag{8}$$

where δ_{i0}' is the sphere velocity of the i^{th} critical contact moment between the rock sphere and the metal plate, m_1 is the mass of the rock, m_2 is the mass of the metal plate, and the damping coefficient of the i th contact-impact is $D_i = ((3K \cdot (1 - e_h^2))/4\delta_{i0}') \cdot \delta^n$.

According to the Lagrange equation, the dynamic model of rock sphere impacting metal plate is given by

$$\frac{\mathrm{d}}{\mathrm{d}t}\left(\frac{\partial T}{\partial \dot{q}_j}\right) - \frac{\partial T}{\partial q_j} + \frac{\partial U}{\partial q_j} = Q_j, \quad (j = 1, 2, \ldots, k). \tag{9}$$

From equation (8), we obtain that

$$\begin{cases} \dfrac{\partial T}{\partial e} = 0, \\ \dfrac{\partial T}{\partial e'} = m_1 e', \\ \dfrac{\mathrm{d}}{\mathrm{d}t}\left(\dfrac{\partial T}{\partial e'}\right) = m_1 e'', \\ \dfrac{\partial U}{\partial e} = -m_1 g. \end{cases} \tag{10}$$

Combined with equations (7), (9), and (10), the relationship of the contact force-energy balance between the rock sphere and the metal plate system in the whole impact-contact process of falling body is obtained as follows:

$$\begin{cases} m_1 e'' - m_1 g = F_n, \\ \dfrac{1}{2} m_1 (e')^2 - m_1 g e - m_2 g h = \displaystyle\int F_n \mathrm{d}\delta. \end{cases} \tag{11}$$

3. Adams Rigid Simulation of Rock Sphere Impacts Metal Plate

3.1. Simulation Model and Parameters Setting. The 3D model of the rock ball impacting the metal plate is established in Solidworks and then is introduced into the Adams dynamics simulation platform, among which the metal plate is supported by four bars. The rock sphere, metal plate, and support bars are rigid bodies, and the dimensions of the rock sphere and metal plate are shown in Table 1. According to Table 1, the properties of the rock sphere and the metal plate

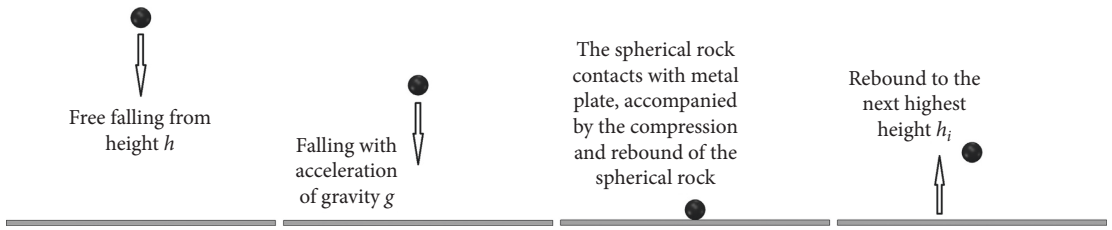

Figure 1: Free-falling impact model.

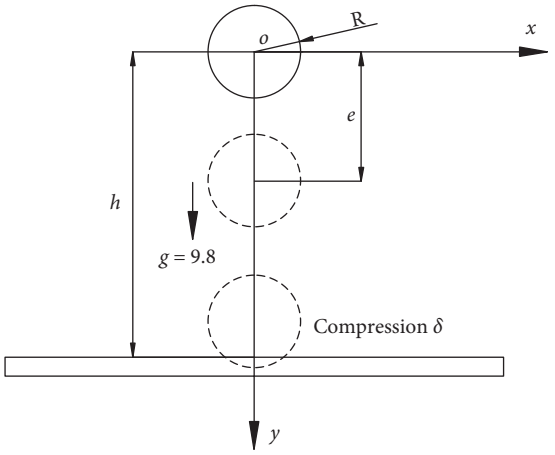

Figure 2: Impact schematic diagram between falling body and plate.

Table 1: Materials properties.

Materials	Density (kg/m^3)	Elastic modulus (Pa)	Poisson's ratio	Size (mm)
Rock sphere	1380	2.26×10^9	0.28	R25
Metal plate	7850	2.1×10^{11}	0.3	$520 \times 420 \times 8$ (outer contour) $458.4 \times 360 \times 8$ (distance of shaft centers)

are defined, respectively, and the system acceleration is set to −9.8 m/s. In addition, the fixed pairs are added between the bottom of the support bars and the ground and between the top of the support bar and the bottom surface of the metal plate, as shown in Figure 3.

Contact stiffness and damping are important parameters to be set in Adams impact simulation. Combined with the data in Table 1, contact stiffness $K = 5.1154524848E \times 108$ is calculated by equations (3) and (4). From [44, 45], the normal force of contact is given by the following relation:

$$F_n = \begin{cases} K \cdot \delta^n + \text{STEP}(\delta, 0, 0, d_{\max}, C_{\max}), & \delta > 0, \\ 0, & \delta \le 0, \end{cases} \quad (12)$$

where $d_{\max}$ is a positive real value specifying the boundary penetration, we set $n = 1.5$ and $d_{\max} = 0.00001$ m, and $C_{\max}$ is the maximum damping coefficient.

The contact problem is solved by the "impact function" in Adams, and it can be expressed in the following form:

$$\text{STEP}(\delta, 0, 0, d_{\max}, C_{\max}) = \begin{cases} 0, & \delta \le 0, \\ C_{\max}\left(\dfrac{\delta}{d_{\max}}\right)^2 \left(3 - \dfrac{2\delta}{d_{\max}}\right), & 0 < \delta < d_{\max}, \\ C_{\max}, & \delta \ge d_{\max}. \end{cases} \quad (13)$$

We know that the damping force is changing in the contact process with the change of δ from equation (5). Khemili and Romdhane [44] consider a damping coefficient that is about one percent of the stiffness coefficient, which lacks the accuracy and theoretical basis, and the damping keeps unchanged in the whole simulation. But in this paper, we assumed that the calculated results by equation (11) is correct and the set value "damping" in Adams is determined by the accurate simulation results which are close to the calculated ones; that is, the "damping" is adjusted to obtain the accurate simulation results.

3.2. Theoretical and Simulation Results. The free-falling body of the rock sphere is defined as a height of 4 m from the center of the rock sphere to the upper surface of the metal plate. The simulation time and simulation step are set up to 5 s and 20,000 steps, respectively. And the theoretical curve for the position of center of the rock sphere is obtained in combination with equation (11). Accordingly, the corresponding simulation results shown in Figure 4 are obtained by adjusting simulation damping.

Figure 4 shows five times of the rebound-impact between the rock sphere and the metal plate. By the adjustment of contact damping, the simulation value of the center position of the rock sphere in the first process of impact is completely consistent with the theoretical value. The initial impact velocity of the second impact decreases in comparison to the previous impact under the action of damping. At the same time, the cumulative error is existed in the software calculating process. Therefore, the simulation value of rebound height of the center of the rock sphere and compression depth of the rock sphere deviates from the theoretical value. What's more, the error between the simulation value of the rebound height and the theoretical value is as high as 10.50% after the fourth impact. And it is 5.7% error between the simulation value and theoretical value of the rock sphere in the maximum compression value during the fifth impact.

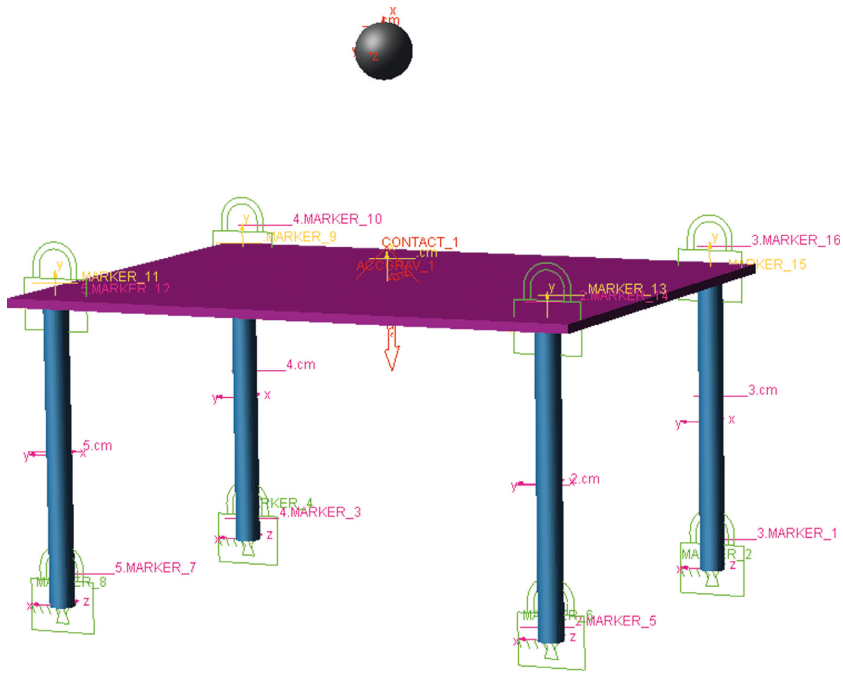

Figure 3: Rigid impact model.

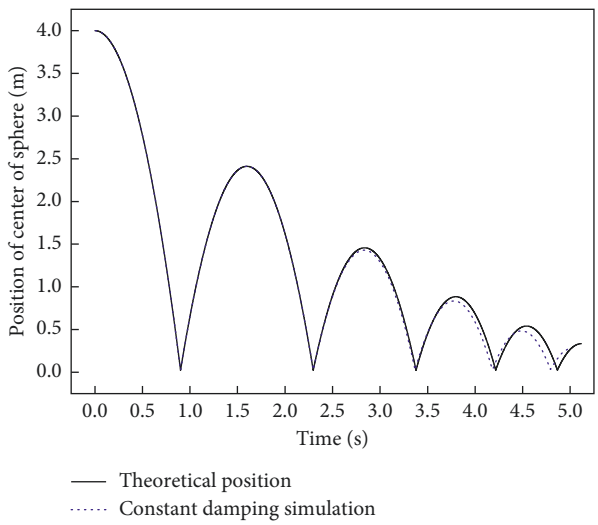

Figure 4: Position of the center of the rock sphere.

The position-time curve in the center of the rock sphere is seriously deviated, and the simulation of the whole process of impact under the settings of constant damping is inaccurate.

The speed of each impact changes during the reciprocating multiple impacts between the rock ball and the metal plate, which results in different damping. Various contact damping are set for different impact processes, respectively, in Adams. And the curves of the theoretical contact response, variable damping simulation, and constant damping simulation are obtained in Figures 5–8, which show the curve of the position of the center of the rock sphere and curves of the impact-contact force, velocity, and acceleration of the rock sphere, respectively.

It can be seen from the figure that the time and value of the variable damping simulation are more closer to the theoretical value than that of the constant damping simulation. The changing speed of impact is taken into consideration. Therefore, by adjusting the damping parameters in each impact process, the simulation position, contact force, velocity, and acceleration of the variable damping impact obtained are almost identical with the corresponding theoretical curves. Taking the maximum compression of the rock sphere (maximum embedded depth) and contact force in each impact as examples, the error ratios between the constant damping simulation and the theoretical value and between the variable damping simulation and the theoretical value in five times of rebound-impact are obtained, respectively, as shown in Table 2. According to the data, the maximum error of the maximum compression of the rock sphere between the simulation and theoretical value is reduced from 7.1653036% to 0.99511% through the variable damping simulation, while the maximum error of the contact force between the variable damping simulation and the theoretical value is reduced from 12.1263013% to 6.3566174%. Compared with the constant damping simulation, the variable damping simulation is more accurate. Therefore, the following research will be conducted based on the method of variable damping simulation. The damping parameter in the five times of impacts of the variable damping simulation is set to 179.75 N·s/m, 172.8 N·s/m, 166.3 N·s/m, 160.9 N·s/m, and 156.5 N·s/m, respectively. Contact damping decreases gradually as the initial impact velocity declines. Based on the variable damping simulation, the relationship between the damping term and the initial impact velocity in Adams simulation (when the rock sphere with 25 mm radius impacts the metal plate and other parameters shown in

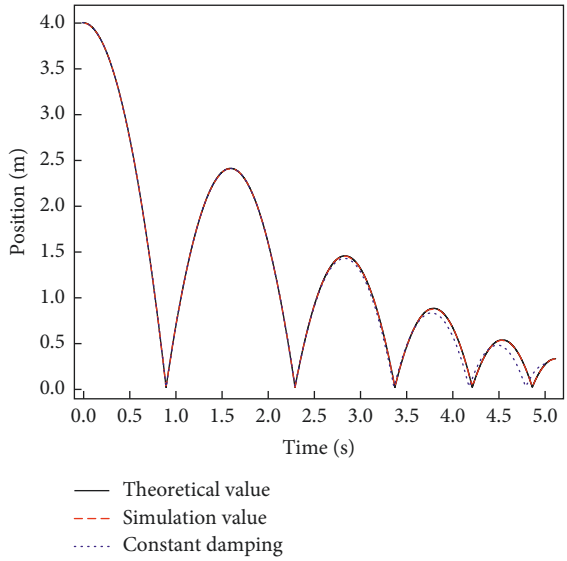

Figure 5: Position of the centroid mass.

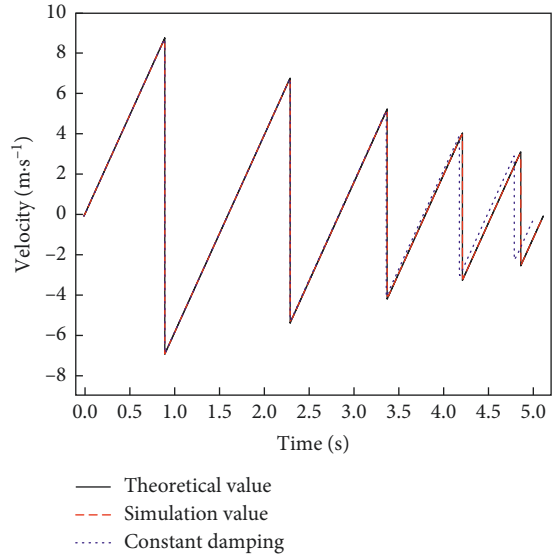

Figure 7: Velocity of centroid mass.

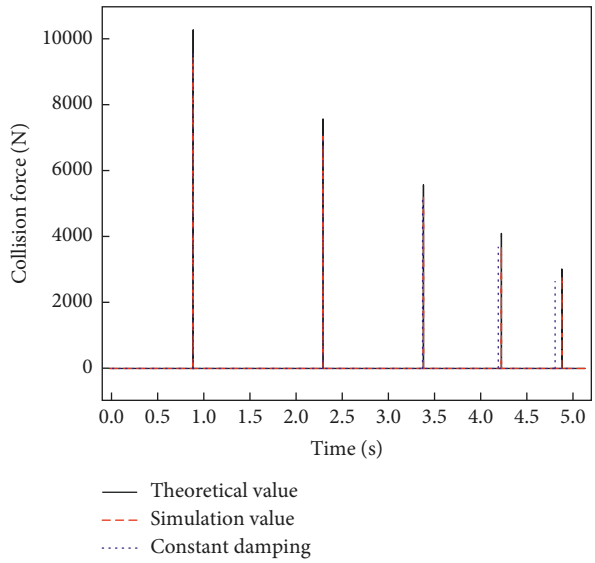

Figure 6: Contact force.

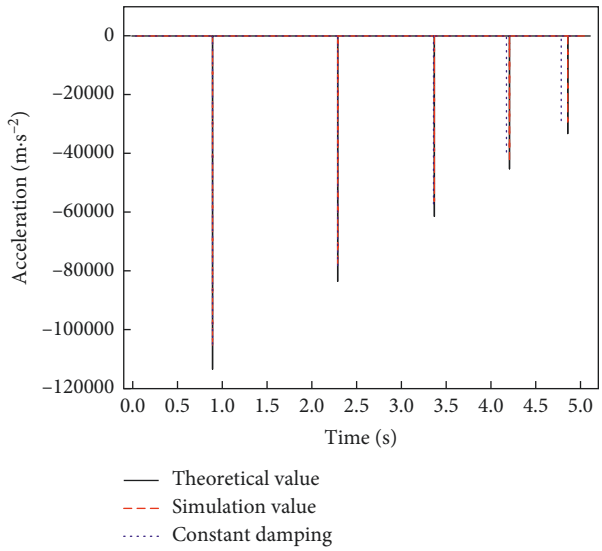

Figure 8: Acceleration of centroid mass.

Table 1) is obtained as follows: $y = 138.93525 + 6.00288v - 0.15582v^2$.

4. Rigid-Flexible Coupling Simulation of Falling Body Impacts Metal Plate

In fact, both rock sphere and metal plate are endowed with elastic properties. However, the falling body impact-contact dynamics model established in the paper and Adams rigid simulation of rock sphere impacts metal plate failure to consider their elastic deformations, which will inevitably lead to the result errors between the theoretical calculation and simulation. Therefore, on the basis of the Adams rigid simulation model, the finite element method and the impact dynamics simulation are combined to conduct the rigid-flexible coupling analysis on the falling body impact model.

The metal plate and rock sphere are meshed by Hypermesh to realize the flexibility of components among which the rock sphere is divided into 499 and 264 grids, while the metal plate is 27,304 grids. In order to ensure the effect of force transmission, the contact area between the lower surface of the metal plate and the supporting bars is defined as a rigid area in Hypermesh. The component grid is shown in Figure 9.

In order to achieve comparative analysis, three kinds of simulations—the rigid simulation of rock ball with impact height of 4 m (as shown in Figure 3), the simulation that the elastic rock sphere impacts rigid plate, and the simulation that the elastic rock sphere impacts elastic plate—are, respectively, carried out in this paper, which are defined as the first type of simulation (Type 1 simulation), the second type of simulation (Type 2 simulation), and the third type of

Table 2: Error between the simulation and theoretical value.

Impact time	Error of compression		Error of contact force	
	Constant damping (%)	Variable damping (%)	Constant damping (%)	Variable damping (%)
First	0.3810047	0.3810047	6.3566174	6.3566174
Second	0.7592313	0.95271	5.7795729	5.2703006
Third	2.2748508	0.8383705	6.7756935	4.7213197
Forth	5.2022971	0.9328795	9.2994821	4.8238711
Fifth	7.1653036	0.0248596	12.1263013	5.3761774

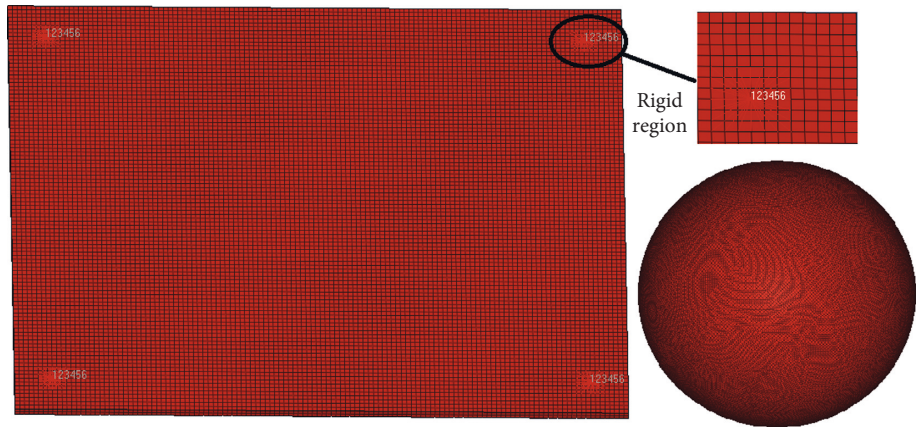

Figure 9: Component grid.

simulation (Type 3 simulation). What's more, Type 2 simulation is based on the rigid simulation model in Adams; accordingly, the rock sphere which is meshed by Hypermesh will be introduced to the model to replace the rigid rock sphere. And in the Type 3 simulation, both rock sphere and metal plate meshed by Hypermesh will be imported to the model to replace the rigid rock ball and the rigid metal plate, respectively. For achieving quantitative comparison, the n^{th} impact damping of the Type 2 simulation and Type 3 simulation is corresponding set as the same as the n^{th} impact damping of the Type 1 simulation, and other parameters are also the same as that of Type 1.

5. Results Discussion and Analysis

5.1. Analysis of Contact Response of Rock Sphere in Three Types of Simulation. Figures 10–13 show the position of the centroid, the contact force, the velocity, and the acceleration curve of the centroid of the rock sphere during the five times of impact between the rock sphere and the metal plate in the three types of simulation.

It can be seen from Figures 10–13 that the position-time and velocity-time curves coincide with each other in the three types of simulation since the rock sphere falls from the height of 4 m to the first contact with the metal plate. Both contact parameters and energy conversion mechanisms change as the changing of the status rock sphere and metal plates in Type 1 simulation, Type 2 simulation, and Type 3 simulation, which further lead to the rock sphere's different compression and energy conversion processes. Then, the rebound height of the rock sphere and reimpact time changes after the first rebound-impact and separation from the metal plate. At the moment of first impact, the initial impact velocity of the rock sphere in the three types of simulation is the same; the contact force and the acceleration of centroid of the rock sphere in the Type 1 simulation are as high as 9583.984 N and 106101 m/s^2, respectively. Since the components of the second and third simulations are flexibly treated, the contact force is reduced to 3582.036 N and 3680.223 N, respectively, while the acceleration of centroid of the rock sphere reduced to 39656 m/s^2 and 40743.3 m/s^2, respectively. After the first impact, rock spheres in the three types of simulations are separated from the metal plates, and the maximum rebound heights present 2.41132 m, 0.26228 m, and 0.18278 m, respectively, among which the rebound height of rock spheres in Type 2 and Type 3 are much lower than Type 1. As a result, in comparison to the Type 1 simulation, the initial impact velocity of the other two is less when the impact occurs again; the contact force and the centroid acceleration of the rock sphere are far less and the impact times are much shorter than Type 1. As the number of the impact increases, the differences ratio of the contact response of the rock spheres between Type 1 and Type 2 and between Type 1 and Type 3 increases due to the cumulative error. Taking five times of impact as examples, the total time of five-time impacts of the Type 2 and Type 3 simulation is less than that of the total time of first two-time impacts of the Type 1 simulation.

From the figures, it also can be known that the initial impact velocity of the rock sphere in the three types of simulations is the same in the first impact, and the maximum contact force produced by the impact between the rock

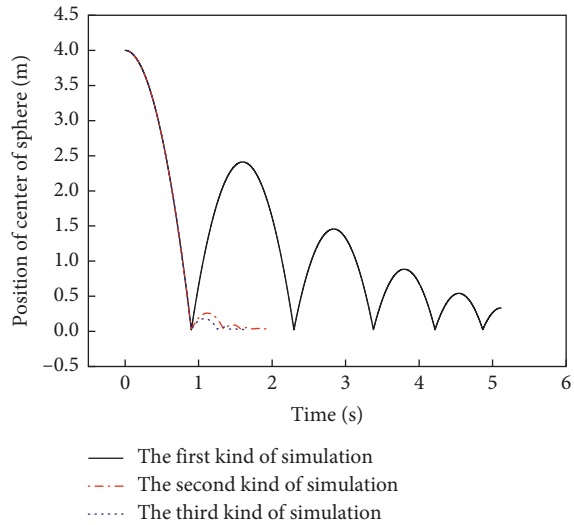

Figure 10: Position of the centroid mass.

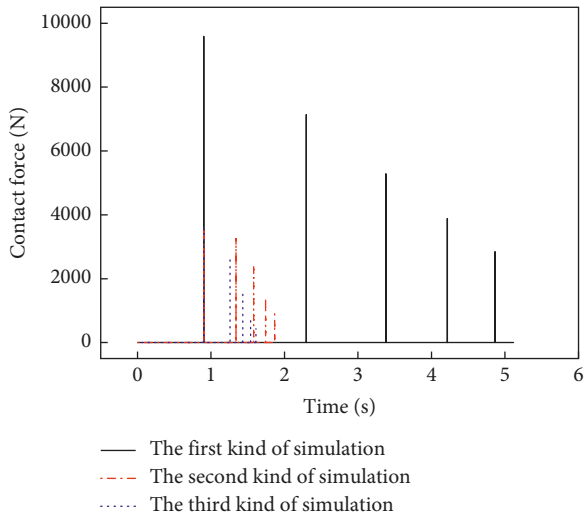

Figure 11: Contact force.

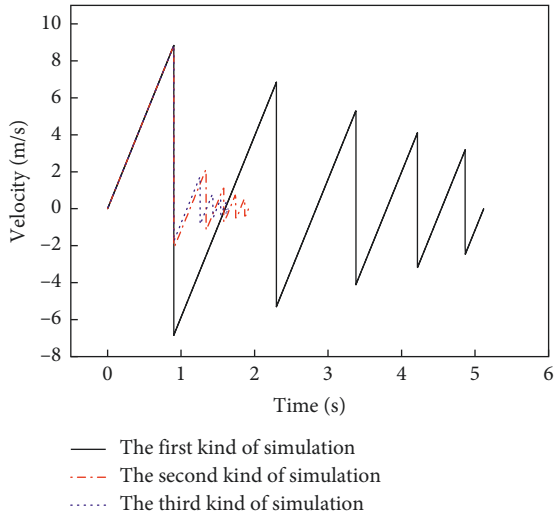

Figure 12: Velocity of centroid mass.

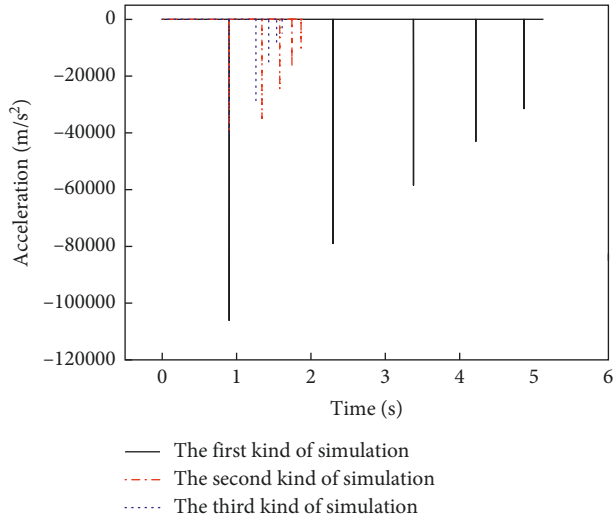

Figure 13: Acceleration of centroid mass.

sphere and the metal plate in the Type 2 simulation is weaker than that of the Type 3. The reason why the rebound height, velocity, and acceleration of the centroid of the rock sphere in the Type 2 simulation are larger than those of the Type 3 lies in that the metal plate in the latter one will absorb energy in the impact-contact process after being flexible. In comparison to the Type 3 simulation, the rebound height of the Type 2 is higher after the first impact. Therefore, the rebound height, the contact force, the velocity, and acceleration of the centroid of the rock sphere in the Type 2 simulation are larger than that of Type 3 during the second to fifth impact, and the rebound time lags behind. Because of the accumulated error, the difference ratio of contact response of the rock sphere is wider with the increase in the impact time.

After the flexible treatment of the impact object, the impact-contact response is much lower than that of the pure rigid impact. Considering more influencing factors, the response law obtained is more accurate than the rigid impact simulation.

5.2. Energy of the Rock Sphere in the Type 2 and 3 Simulations. In the process of rock sphere falling and its impact on the metal plate, transformation and transmission are generated in the system energy. The Type 1 simulation belongs to the pure rigid impact, while the Type 2 and Type 3 are accompanied by the elastic deformation of the rock sphere. Four curves of the kinetic energy, potential energy, strain energy, and rotational energy of rock spheres in the Type 2 and Type 3 simulations are shown in Figures 14–17.

Every initial position of the rock sphere during the five times of impact is considered as the zero potential energy point. It can be known that the relative change in potential energy of the rock sphere decreases gradually with the increase in the impact time, which is because the rebound height of the rock sphere decreases gradually after each impact as the impact performs. At the end of each impact, the rebound height of the rock sphere gradually decreases. And the diminution of potential energy leads to the decrease

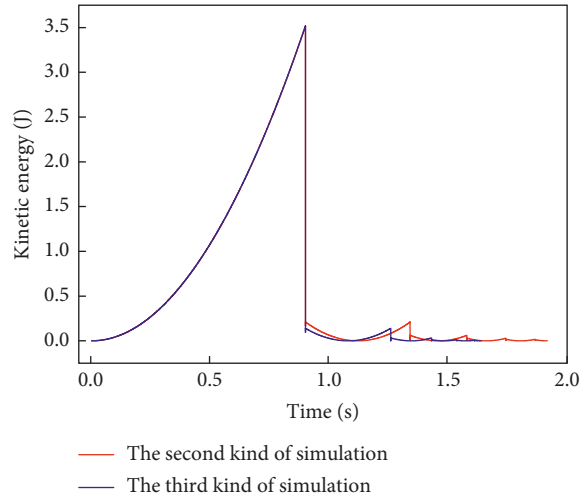

Figure 14: Kinetic energy.

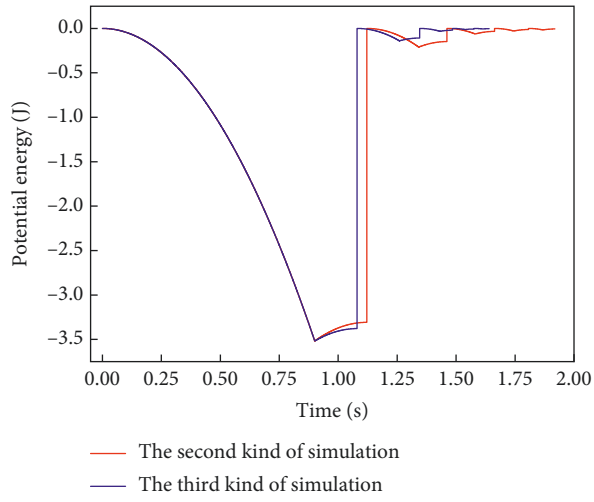

Figure 15: Potential energy.

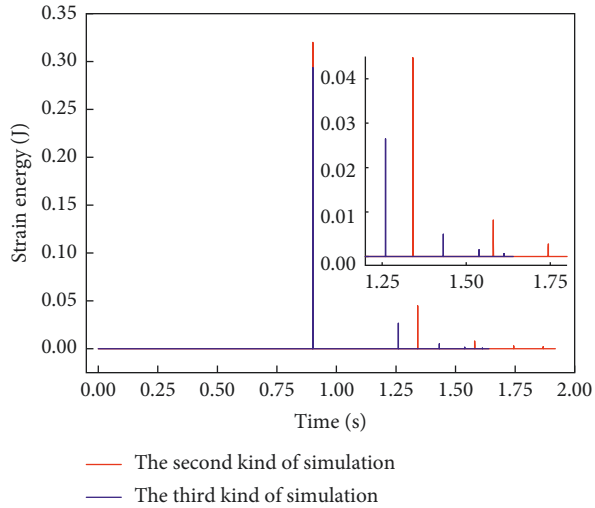

Figure 16: Strain energy.

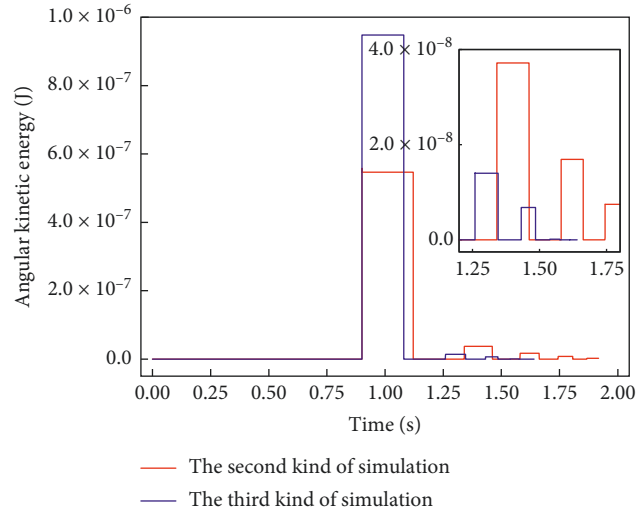

Figure 17: Angular kinetic energy.

in the other energy which is transferred to other parts. It is known from the figures that, with the increase in the impact time, the maximum kinetic energy, the maximum strain energy, and the maximum rotational energy of the rock sphere are gradually reduced during each impact. Five times of the impact simulation in the whole process are conducted independently; therefore, the energy variation tendency of each part of the rock sphere is as same as that of the first impact.

The energy of each part of the rock sphere during the first impact can utilized as an example. From the initial drop to the first impact, the maximum relative change in potential energy of the rock sphere in Type 2 simulation is 3.51799 J, and the initial kinetic energy of the rock sphere at the initial contact time is 3.51785 J. At the moment of impact, the kinetic energy of the rock ball drops to zero rapidly, and then it is separated from the metal plate by the energy of 0.21011 J. The residual kinetic energy occupies less than 6% of the maximum relative change in potential energy of the rock sphere. And the maximum elastic strain energy of the rock sphere during compression is 0.32 J, which only accounts for 9.1% of the maximum relative change in potential energy. The kinetic energy of the rock sphere includes the translational kinetic energy and the rotational energy. Only the vertical impact between the rock ball and the metal plate is considered in the simulation, and no friction and other parameters is set. The rotation of rock sphere after the impact is mainly caused by the calculation error of the simulation software. It can be neglected that its rotation energy is less than 10^{-6} and the maximum rotation energy is less than 6×10^{-7} J. In the Type 3 simulation, the maximum relative change in potential energy of the rock sphere shows 3.51801 J. The initial kinetic energy of the rock sphere at the initial contact time is 3.51786 J, the kinetic energy of the rock sphere drops to zero rapidly, and then it is separated from the metal plate by the energy of 0.13997 J. The residual kinetic energy accounts for less than 4% of the maximum relative change in potential energy of the rock sphere. The maximum elastic strain energy of the rock sphere

compression is 0.2935 J, which only accounts for 9.3%. In addition, the maximum rotational energy is less than 10^{-6} J, which also can be ignored.

Two types of simulation are the same in change law of the energy manifestations during five times of impact. After the impact, the rock sphere's rebound height in Type 2 is greater than Type 3, which causes the maximum relative change in potential energy, the maximum residual kinetic energy, and the strain energy of the rock sphere also to be greater. Elastic deformation appears in the rock sphere and the metal plate in the Type 3 simulation, resulting in the rotation energy in the third type is greater than that in the second type. As the times of impacts increases and due to the existence of cumulative error, the difference in the energy between the two types of simulation increases gradually. At the same time, it can be analyzed that only a few of rock potential energy is transformed into the rock sphere's own energy after the treatment of flexibility, and the rest energy is dissipated by the system impact. Although the energy difference between the two types of simulations is relatively small, the results of Type 3 are more realistic and credible in comparison to that of Type 2, which is because the former considers the deformation energy absorption of the metal plate after the flexible treatment of the metal plate.

5.3. Vibration Response of the Metal Plate in Type 3 Simulation. The metal plate belongs to the macroscopic 3D thin plate. As a result, after the flexible treatment of the plate, not only the elastic deformation of the rock sphere appears in the system but also the vibration-impact response is generated in the metal plate. Figures 18–23 show the vibration response and energy variation curve of the metal plate after impact.

As shown in the figure, the centroid of the metal plate vibrates up and down around the initial position after being impacted by the rock sphere, the potential energy vibrates around the zero potential energy point, and the velocity and acceleration also present reciprocating vibration. Due to the influence parameters such as the system damping, the vibration response of the metal plate decreases gradually with the increase in the time of impact. Under the impact of rock sphere with the radius of 25 mm and velocity of 8.85 m/s, the maximum displacement of the centroid of the metal plate shows 10^{-4} m, which is about 1.25% of the thickness of the metal plate. The maximum velocity of the center of mass reaches 0.1 m/s, and the maximum acceleration of the center of mass reaches 200 m/s^2. With the increase in the time of impact, the displacement and velocity of the center of mass decrease fasters while the maximum acceleration decreases slower. The maximum acceleration of the center of mass is still over 31 m/s^2 in the fifth impact, and the vibration response of the acceleration is remarkable. Therefore, the acceleration can be taken as the target parameter, and the vibration acceleration signal of the metal plate can be obtained by using high-precision acceleration sensor to achieve experimental analysis. In addition, velocity can also be used as the target parameter for data analysis when conducting the experiment. The maximum relative change in potential

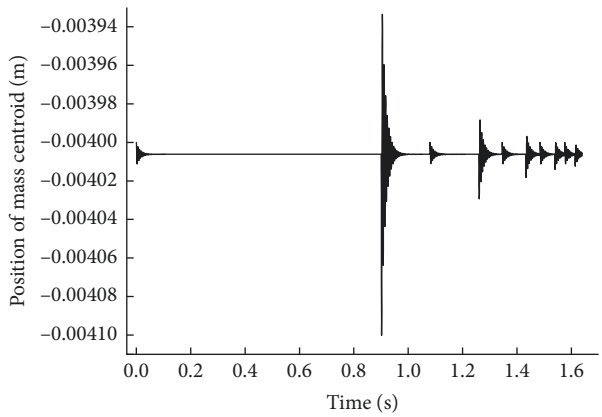

Figure 18: Centroid position of the metal plate.

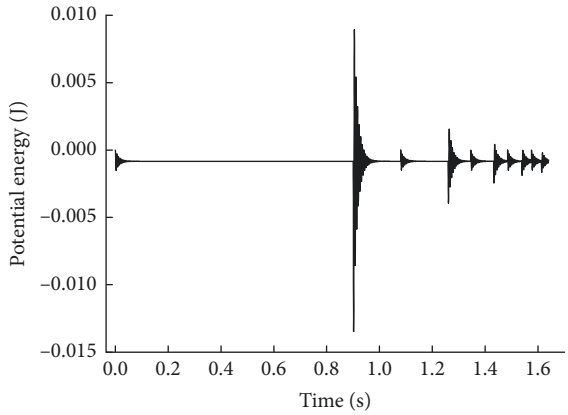

Figure 19: Change in potential energy.

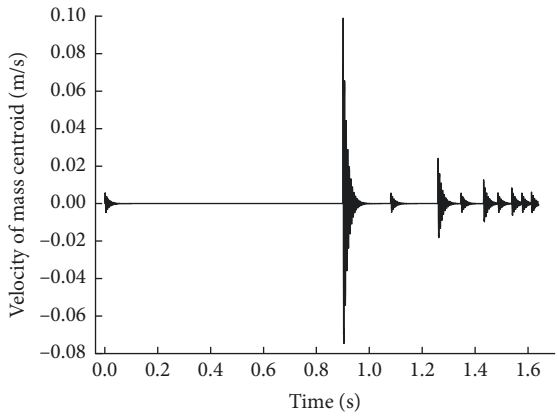

Figure 20: Centroid velocity of the metal plate.

energy of the metal plate is less than 0.015 J, and the potential energy changes slightly. The maximum kinetic energy of the metal plate is 0.29412 J, which accounts for 8.36% of the maximum relative change in potential energy of the rock sphere. And its maximum strain energy is 0.13225 J, which accounts for 3.76% of the maximum relative change in potential energy of the rock sphere. When the elastic rock sphere impacts on the elastic metal plate, the total energy of

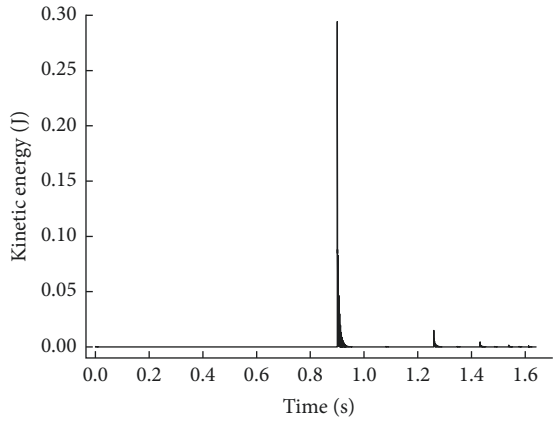

Figure 21: Kinetic energy of the metal plate.

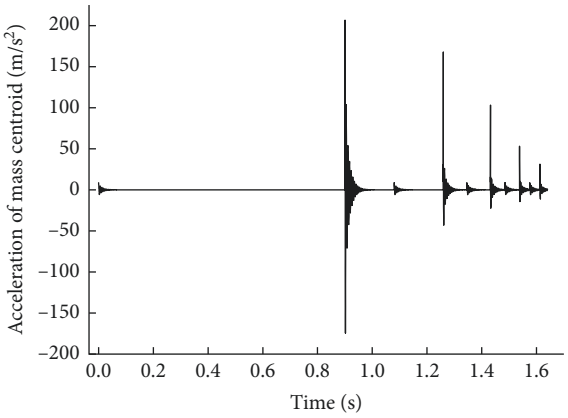

Figure 22: Centroid acceleration of the metal plate.

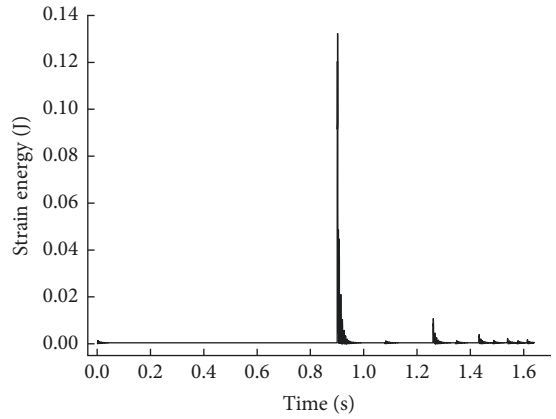

Figure 23: Strain energy of the metal plate.

the metal plate accounts for more than 11% of the maximum potential energy change of rock sphere and it cannot be ignored. Otherwise, it is inaccurate to predict the contact response. The flexible deformation of the metal plate is a factor that must be considered in the impact-contact between the rock sphere and the metal thin plate. Compared with the first impact, the maximum kinetic energy and strain energy of the metal plate are greatly reduced in the second impact. Combined with the energy conversion in the Type 3 simulation of the rock sphere, most energy of the system is consumed when the rock sphere and metal plate are flexibly treated.

6. Conclusions

Based on the Hertz's contact theory, L-N contact model, and the analysis of repeated impact that the object falls freely and impacts the metal plate, this paper establishes the dynamics model that the rock sphere impacts metal plate in combination with the Lagrange equation. By the comparative analysis between the rigid constant and variable damping simulation and the theoretical results, the functional relationship between damping term and the initial impact velocity in Adams simulation is achieved. On the basis of variable damping simulation, this paper also combines Adams with Hypermesh to conduct three types of simulations when rock sphere falls freely from a height 4 m and impacts the metal plate, which are the rigid simulation of rock sphere impacts metal plate, the simulation elastic rock sphere impacts the rigid metal plate, and the simulation that the elastic rock sphere impacts the elastic metal plate. The results are concluded as following:

(1) The dynamics model of the rock sphere impacting the metal plate is established in this paper. In addition, this paper puts forward that the method of variable damping simulation can be utilized to study the vibration response of the rock sphere and the metal plate in vertical reciprocating impact. Compared with the constant damping simulation, the maximum error of the maximum compression of the rock sphere and the contact force between the simulation and theoretical values decreases from 7.1653036% and 12.1263013% to 0.95271% and 6.3566174%, respectively. The rigid simulation of variable damping is more consistent with the theoretical results, and the variable damping simulation is more accurate.

(2) According to the theoretical model established in this paper, the damping of five times of impact in the rigid impact simulation is 179.75 N·s/m, 172.8 N·s/m, 166.3 N·s/m, 160.9 N·s/m, and 156.5 N·s/m, respectively. Based on the data, this paper first proposes the functional relationship between the contact damping term and the initial impact-contact velocity in the Adams simulation platform. Under the conditions described above, the function can be expressed as $y = 138.93525 + 6.00288v - 0.15582v^2$.

(3) Under the same damping settings and after the flexibility treatment of the impact object (Type 2 and 3 simulations), the impact-contact responses such as the displacement of the center of mass, the contact force, the velocity, and the acceleration of the center of mass of the rock sphere are greatly reduced. Further influencing factors are considered. Therefore, the response law is more precise compared with the rigid impact simulation.

(4) Compared with the Type 2 simulation, the impact-contact responses in the Type 3 simulation such as the displacement of mass center, the contact force, the velocity, and the acceleration of mass center decreases greatly due to the consideration of the elastic deformation of the metal plate and its energy absorption. Besides, the rotational energy, the kinetic energy, the relative variation of potential energy, and strain energy of rock sphere decrease after the impact, except for the rotation of the rock sphere.

(5) After the impact, the vibration response such as the centroid speed and acceleration of the metal plate is significant. Therefore, the velocity and acceleration can be utilized as the target parameters. In the actual experiment, these two vibration signals of the metal plate can be obtained for analysis by the high-precision acceleration sensor or other facilities.

(6) After being impacted by the rock sphere, the total energy of the metal plate accounts for more than 11% of the maximum relative change in potential energy of the rock sphere. The theoretical and simulation methods for studying the contact response between the particles and the metal plate impact are inaccurate without considering the deflection and energy absorption of the metal plate. After the flexible treatment of the rock sphere and the metal plate, most energy in the system is consumed during the impact, and only a part of it is transformed to the energy of the rock sphere and the metal plate.

The conclusion of this paper will provide a theoretical calculation method for vertical reciprocating impact between objects, the theoretical basis for setting the damping term in Adams simulation, variable damping simulation method for continuous impact-contact of medium, and target measurement parameters for the experimental test. In addition, it will support research basis for the impact behavior between the coal gangue particles and the metal plate in the process of coal gangue caving and the realization of automatic mining technology.

Data Availability

The data used to support the findings of this study are included within the article and are available from the corresponding author upon request.

Conflicts of Interest

The authors declare that there are no conflicts of interest.

Acknowledgments

This work was supported by the National Natural Science Fund of China (Grant nos. 51674155 and 51974170), Innovative Team Development Project of Ministry of Education (Grant no. IRT_16R45), Special Funds for Climbing Project of Taishan Scholars, National Natural Science Fund of Shandong Province (Grant no. ZR2019BEE066), Postgraduate Science and Technology Innovation Project of Shandong University of Science and Technology (Grant no. SDKDYC190108), Youth Education Scientific Planning Projects of Shandong Province-Academic Projects of the college students (19BSH099), and College of Mechanical and Electronic Engineering student science and technology innovation team in Shandong University of Science and Technology (ZD201901).

References

[1] Y. Yang, Q. Zeng, and L. Wan, "Dynamic response analysis of the vertical elastic impact of the spherical rock on the metal plate," *International Journal of Solids and Structures*, vol. 158, pp. 287–302, 2019.

[2] Y. Du and S. Wang, "Energy dissipation in normal elasto-plastic impact between two spheres," *Journal of Applied Mechanics*, vol. 76, no. 6, pp. 1089–1094, 2009.

[3] C. Thornton, Z. Ning, W. Chuan-yu, M. Nasrullah, and L. Long-yuan, "Contact mechanics and coefficients of restitution," *Granular Gases*, vol. 564, pp. 184–194, 2001.

[4] H. Minamoto and S. Kawamura, "Moderately high speed impact of two identical spheres," *International Journal of Impact Engineering*, vol. 38, no. 2-3, pp. 123–129, 2011.

[5] M. R. W. Brake, "An analytical elastic plastic contact model with strain hardening and frictional effects for normal and oblique impacts," *International Journal of Solids and Structures*, vol. 62, pp. 104–123, 2015.

[6] V. Brizmer, Y. Kligerman, and I. Etsion, "The effect of contact conditions and material properties on the elasticity terminus of a spherical contact," *International Journal of Solids and Structures*, vol. 43, no. 18-19, pp. 5736–5749, 2006.

[7] R. Goltsberg and I. Etsion, "Contact area and maximum equivalent stress in elastic spherical contact with thin hard coating," *Tribology International*, vol. 93, pp. 289–296, 2016.

[8] W. J. Stronge and A. D. C. Ashcroft, "Oblique impact of inflated balls at large deflections," *International Journal of Impact Engineering*, vol. 34, no. 6, pp. 1003–1019, 2007.

[9] C. Thornton, S. J. Cummins, and P. W. Cleary, "On elastic-plastic normal contact force models, with and without adhesion," *Powder Technology*, vol. 315, pp. 339–346, 2017.

[10] H. Xiao, M. J. Brennan, and Y. Shao, "On the undamped free vibration of a mass interacting with a Hertzian contact stiffness," *Mechanics Research Communications*, vol. 38, no. 8, pp. 560–564, 2011.

[11] E. Willert, S. Kusche, and V. L. Popov, "The influence of viscoelasticity on velocity-dependent restitutions in the oblique impact of spheres," *Facta Universitatis, Series: Mechanical Engineering*, vol. 15, no. 2, pp. 269–284, 2017.

[12] J. Jäger, "Properties of equal bodies in contact with friction," *International Journal of Solids and Structures*, vol. 40, no. 19, pp. 5051–5061, 2003.

[13] C.-Y. Wu, L.-Y. Li, and C. Thornton, "Rebound behaviour of spheres for plastic impacts," *International Journal of Impact Engineering*, vol. 28, no. 9, pp. 929–946, 2003.

[14] L. Vu-Quoc, L. Lesburg, and X. Zhang, "An accurate tangential force-displacement model for granular-flow simulations: contacting spheres with plastic deformation, force-driven formulation," *Journal of Computational Physics*, vol. 196, no. 1, pp. 298–326, 2004.

[15] J. Y. Wang, Z. Y. Liu, and J. Z. Hong, "Influence of non-physical chosen parameters on impact dynamics of discretized

elastic bodies," *Journal of Mechanics*, vol. 35, no. 02, pp. 167–177, 2019.

[16] P. Peng, C. Di, L. Qian, and G. Chen, "Parameter identification and experimental investigation of sphere-plane contact impact dynamics," *Experimental Techniques*, vol. 41, no. 5, pp. 547–555, 2017.

[17] C.-S. Liu, K. Zhang, and R. Yang, "The FEM analysis and approximate model for cylindrical joints with clearances," *Mechanism and Machine Theory*, vol. 42, no. 2, pp. 183–197, 2007.

[18] Y. Yang, Q. Zeng, and L. Wan, "Contact response analysis of vertical impact between elastic sphere and elastic half space," *Shock and Vibration*, vol. 2018, Article ID 1802174, 15 pages, 2018.

[19] J.-P. Mougin, P. Perrotin, M. Mommessin, J. Tonnelo, and A. Agbossou, "Rock fall impact on reinforced concrete slab: an experimental approach," *International Journal of Impact Engineering*, vol. 31, no. 2, pp. 169–183, 2005.

[20] H. Minamoto and S. Kawamura, "Effects of material strain rate sensitivity in low speed impact between two identical spheres," *International Journal of Impact Engineering*, vol. 36, no. 5, pp. 680–686, 2009.

[21] E. Olsson and P.-L. Larsson, "On the tangential contact behavior at elastic-plastic spherical contact problems," *Wear*, vol. 319, no. 1-2, pp. 110–117, 2014.

[22] J. Xie, M. Dong, S. Li, Y. Shang, and Z. Fu, "Dynamic characteristics for the normal impact process of micro-particles with a flat surface," *Aerosol Science and Technology*, vol. 52, no. 2, pp. 222–233, 2017.

[23] E. Willert, I. A. Lyashenko, and V. L. Popov, "Influence of the Tabor parameter on the adhesive normal impact of spheres in Maugis-Dugdale approximation," *Computational Particle Mechanics*, vol. 5, no. 3, pp. 313–318, 2017.

[24] T. Wang, L. Wang, L. Gu, and D. Zheng, "Stress analysis of elastic coated solids in point contact," *Tribology International*, vol. 86, pp. 52–61, 2015.

[25] Z. Wang, H. Yu, and Q. Wang, "Layer-substrate system with an imperfectly bonded interface: spring-like condition," *International Journal of Mechanical Sciences*, vol. 134, pp. 315–335, 2017.

[26] R. L. Jackson, I. Green, and D. B. Marghitu, "Predicting the coefficient of restitution of impacting elastic-perfectly plastic spheres," *Nonlinear Dynamics*, vol. 60, no. 3, pp. 217–229, 2010.

[27] B. Zhao, S. Zhang, and L. M. Keer, "Spherical elastic-plastic contact model for power-law hardening materials under combined normal and tangential loads," *Journal of Tribology*, vol. 139, no. 2, Article ID 021401, 2017.

[28] C. Thornton, "Coefficient of restitution for collinear collisions of elastic-perfectly plastic spheres," *Journal of Applied Mechanics*, vol. 64, no. 2, pp. 383–386, 1997.

[29] J. Jamari and D. J. Schipper, "An elastic-plastic contact model of ellipsoid bodies," *Tribology Letters*, vol. 21, no. 3, pp. 262–271, 2006.

[30] Y. Du and S. L. Wang, "Elastoplastic normal impact dissipation model of two particles," *Chinese Journal of Mechanical Engineering*, vol. 45, no. 02, pp. 149–156, 2009.

[31] L. Vu-Quoc, X. Zhang, and L. Lesburg, "Normal and tangential force-displacement relations for frictional elasto-plastic contact of spheres," *International Journal of Solids and Structures*, vol. 38, no. 36-37, pp. 6455–6489, 2001.

[32] S. He, Y. Wu, and X. Li, "Theoretical model on elastic-plastic granule impact," *Engineering Mechanics*, vol. 25, no. 12, pp. 19–24, 2008.

[33] S. Krijt, C. Güttler, D. Heißelmann, C. Dominik, and A. G. G. M. Tielens, "Energy dissipation in head-on collisions of spheres," *Journal of Physics D: Applied Physics*, vol. 46, no. 43, pp. 435303–435314, 2013.

[34] Y. Kligerman, Y. Kadin, and I. Etsion, "Unloading of an elastic-plastic loaded spherical contact," in *Proceedings of the 2004 AIMETA International Tribology Conference*, vol. 42, no. 13, pp. 183–190, Long Beach, CA, USA, October 2004.

[35] A. Ovcharenko, G. Halperin, G. Verberne, and I. Etsion, "In situ investigation of the contact area in elastic-plastic spherical contact during loading-unloading," *Tribology Letters*, vol. 25, no. 2, pp. 153–160, 2007.

[36] Q. Zeng, Y. Yang, X. Zhang, L. Wan, J. Zhou, and G. Yin, "Study on metal plate vibration response under coal-gangue impact based on 3D simulation," *Arabian Journal for Science and Engineering*, vol. 44, no. 9, pp. 7567–7580, 2019.

[37] O. Cermik, H. Ghaednia, and D. B. Marghitu, "Analytical study of the oblique impact of an elastic sphere with a rigid flat," in *Acoustics and Vibration of Mechanical Structures*, pp. 33–40, Springer Proceedings in Physics, Springer, New York, NY, USA, 2018.

[38] Y. Yang, Q. L. Zeng, L. R. Wan, and G. J. Yin, "Vibration test of single coal gangue particle directly impacting the metal plate and the study of coal gangue recognition based on vibration signal and stacking integration," *IEEE ACCESS*, vol. 7, pp. 106984–106805, 2019.

[39] Y. Kadin, Y. Kligerman, and I. Etsion, "Multiple loading-unloading of an elastic-plastic spherical contact," *International Journal of Solids and Structures*, vol. 43, no. 22-23, pp. 7119–7127, 2006.

[40] Y. Kadin, Y. Kligerman, and I. Etsion, "Cyclic loading of an elastic-plastic adhesive spherical microcontact," *Journal of Applied Physics*, vol. 104, no. 7, Article ID 073522, 2008.

[41] K. L. Johnson, *Contact Mechanics*, Cambridge University Press, Cambridge, UK, 1985.

[42] H. M. Lankarani and P. E. Nikravesh, "A contact force model with hysteresis damping for impact analysis of multibody systems," *Journal of Mechanical Design*, vol. 112, no. 3, pp. 369–376, 1990.

[43] H. M. Lankarani and P. E. Nikravesh, "Continuous contact force models for impact analysis in multibody systems," *Nonlinear Dynamics*, vol. 5, no. 2, pp. 193–207, 1994.

[44] I. Khemili and L. Romdhane, "Dynamic analysis of a flexible slider-crank mechanism with clearance," *European Journal of Mechanics—A/Solids*, vol. 27, no. 5, pp. 882–898, 2008.

[45] M. A. B. Abdallah, I. Khemili, and N. Aifaoui, "Numerical investigation of a flexible slider–crank mechanism with multijoints with clearance," *Multibody System Dynamics*, vol. 38, no. 2, pp. 173–199, 2016.